

Oxygen K-edge in vanadium oxides: simulations and experiments

C. Hébert^{1,a}, M. Willinger^{1,2}, D.S. Su², P. Pongratz¹, P. Schattschneider¹, and R. Schlögl²

¹ Institut für Festkörper Physik, Technische Universität Wien, Wiedner Hauptstrasse 8-10 1040 Wien, Austria

² Department of Inorganic Chemistry, Fritz Haber Institute of the Max Planck Society, Faradayweg 4-6, 14195 Berlin, Germany

Received 17 December 2001 / Received in final form 19 June 2002

Published online 13 August 2002 – © EDP Sciences, Società Italiana di Fisica, Springer-Verlag 2002

Abstract. Band-structure (BS) calculations of the density of states (DOS) using the full potential augmented plane waves code WIEN97 were performed on the four single-valence vanadium oxides VO, V₂O₃, VO₂ and V₂O₅. The DOS are discussed with respect to the distortions of the VO₆ octahedra, the oxidation states of vanadium and the orbital hybridisations of oxygen atoms. The simulated oxygen K-edge fine structures (ELNES) calculated with the TELNES program were compared with experimental results obtained by electron energy-loss spectrometry (EELS), showing good agreement. We show that changes in the fine structures of the investigated vanadium oxides mainly result from changes in the O-*p* DOS and not from the shift of the DOS according to a rigid band model.

PACS. 79.20.Uv Electron energy loss spectroscopy – 71.20.-b Electron density of states and band structure of crystalline solids – 71.20.Be Transition metals and alloys – 71.15.Ap Basis sets (plane-wave, APS, LCAO, etc.) and related methodology (scattering methods, ASA, linearized methods)

1 Introduction

Among the various oxides of vanadium, there are four (VO, V₂O₃, VO₂ and V₂O₅) in which vanadium is in a single valence state, *i.e.*, in V²⁺, V³⁺, V⁴⁺ and V⁵⁺, respectively. These oxides merit special attention because of their outstanding structural flexibility combined with chemical and physical properties which are of interest for catalytic and electrochemical applications. For instance, VO is a metal with rock-salt structure. V₂O₃ is in a paramagnetic metallic phase with corundum structure (α -Al₂O₃) above 165 K and an antiferromagnetic insulator with monoclinic structure below [1,2]. VO₂ undergoes a first order transition from a diamagnetic semiconductor phase below 340 K to a paramagnetic metallic state with rutile structure above 340 K [1,3]. V₂O₅ is a diamagnetic insulator at room temperature [1] with orthorhombic structure. V₂O₅ is an essential ingredient to heterogeneous catalysis widely used in a variety of chemical reactions, such as in partial oxidation reactions or in the selective reduction of NO_x. The mentioned single valence vanadium oxides exist beside of a wide variety of mixed valence oxides in which vanadium atoms exist in at least two of the above mentioned valence states. Such mixed valence oxides are found to be thermodynamically stable and can be synthesised by various methods or can be formed as intermediate phases in catalytic reactions.

The variability of the vanadium-oxygen system in electronic properties calls for a sensitive and spatially resolv-

ing analytical methodology for investigation of structure-function relationship. ELNES (energy loss near edge structures) analysis performed in an analytical transmission electron microscope (TEM) gives the necessary information provided that a safe understanding of the spectral features is available. To this end an analysis of spectral properties of reference oxides is presented here.

Numerous theoretical investigations have been performed on vanadium oxides [4–10]. More recently two calculations have been performed on V₂O₅ within the density functional theory: Eyert *et al.* concentrated on the role of the deformation of the VO₆ octahedron on the DOS using an augmented spherical wave approach within the local density approximation [11], and Chakrabarati *et al.* studied the bulk and (010) surface of V₂O₅ using the full potential augmented plane wave code WIEN97 [12]. In a study of bulk and surface properties of vanadium and molybdenum oxides Hermann and Witko showed the total DOS of V₂O₅, VO₂ and V₂O₃ calculated with the WIEN97 code [13]. Experimentally, oxygen K near edge structures have been studied by Abe *et al.*, by means of EELS showing the metal-insulator transition in VO₂ [3]. O K-edges in V₂O₅, VO₂, V₂O₃ are shown by Lin *et al.* measured by ELNES [14] and Abbate *et al.* recorded in X-ray Absorption Spectroscopy (XAS) [1]. Despite the fact that much work was carried out, the different theoretical investigations were made with different methods and thus different types and levels of approximation. Therefore there is still need for a systematic investigation of single valence vanadium oxides with the same

^a e-mail: cecile.hebert@tuwien.ac.at

Table 1. Structures of the simulated and observed compounds. Lattice parameters are given in Å. Data were taken from [22] for V₂O₅, from [4] for VO₂, from [23] for V₂O₃ and from [24] for VO. The V-O distances are also given.

	Space group	lattice parameters (Å)	α	atom positions	V-O distances (Å)
V ₂ O ₅	Pmmn (59) orthorhombic	$a = 11.512$		V (4 <i>f</i>) $x = 0.10118$ $z = 0.8917$	
		$b = 3.564$		O(1) (4 <i>f</i>) $x = 0.1043$ $z = 0.531$	1.57; 2.79
		$c = 4.368$		O(2) (2 <i>a</i>) $z = 0.001$	1.78
				O(3) (4 <i>f</i>) $x = 0.9311$ $z = 0.003$	1.88; 2.02
VO ₂	P4 ₂ /mm (136) tetragonal	$a = 4.5546$		V (2 <i>a</i>)	
		$c = 2.8514$		O (4 <i>f</i>) $x = 0.3$	1.921; 1.932
V ₂ O ₃	R $\bar{3}$ c (167) rhombohedral	$a = 5.4734$	53.78°	V (4 <i>c</i>) $x = 0.34629$	
				O (6 <i>e</i>) $x = 0.9382$	1.97; 2.05
VO	Fm $\bar{3}$ m (225) cubic	$a = 4.12$		V (4 <i>a</i>)	
				O (4 <i>b</i>)	2.06

theoretical and experimental tools. Also no direct comparison of the DOS of these four compounds has been done.

In the present work, we give a comprehensive investigation of the variation in the O-K ELNES with oxidation state in the four important single valence vanadium oxides, VO, V₂O₃, VO₂ and V₂O₅. This knowledge can help us to understand the electronic structure of all the other vanadium oxides with intermediate oxidation states. For a reliable comparison, all the band structure calculations were performed with the same programme code and discussed with emphasis on the density of unoccupied states. The oxygen K-edges from the four oxides are extracted from EELS spectra recorded with the same transmission electron microscope under comparable experimental conditions.

2 Method

In the TEM fast incoming electrons (typically between 100 and 400 keV) lose energy due to a variety of interactions with the sample [15]. One possible process is the excitation of a core electron, a process similar to the one occurring in XAS. Modern energy spectrometers or filters in the TEM such as the PEELS, the GIF or in-column filters can resolve 0.5 to 1 eV. In combination with a field emission source, these instruments are sufficiently sensitive to detect faint variations in the ELNES. Methods for the calculations of those fine structures were reviewed by Rez *et al.* [16,17].

In a band structure approach ELNES is calculated within the first Born-approximation under the assumption that the incoming and outgoing fast electrons are plane waves with wave vectors \mathbf{k}_i and \mathbf{k}_f . The double differential cross-section for inelastic electron scattering is related to the Dynamic Form Factor (DFF) [18] as:

$$\frac{\partial^2 \sigma}{\partial \Omega \partial E} = \left[\frac{4\gamma^2}{a_0^2 q^4} \right] \frac{k_f}{k_i} \text{DFF}(\mathbf{q}, E) \quad (1)$$

where $\mathbf{q} = \mathbf{k}_i - \mathbf{k}_f$ is the momentum transfer, a_0 the Bohr radius, E the energy and $\gamma = \sqrt{1 - \beta^2}$ is the relativistic factor. The DFF is given by:

$$\text{DFF}(\mathbf{q}, E) = \sum_{i,f} |\langle i | e^{i\mathbf{q}\cdot\mathbf{r}} | f \rangle|^2 \delta(E + E_i - E_f). \quad (2)$$

The summation is done over all occupied initial and empty final states $\langle i |$ and $| f \rangle$.

If we consider a core loss in a crystal, the initial state is represented by an atomic core state and the final state by a Bloch wave which can be projected onto a basis set of atomic orbitals. If additionally the sample is polycrystalline and thus the DFF can be integrated over all directions of \mathbf{q} , the DFF is given by [19]:

$$\text{DFF}(\mathbf{q}, E) = o_l \sum_{\lambda=0}^{\infty} \sum_{l'=|l-\lambda|}^{l+\lambda} \chi_{l'}^t(\varepsilon') \times (2\lambda + 1) \times \begin{pmatrix} l & \lambda & l' \\ 0 & 0 & 0 \end{pmatrix}^2 \langle j_\lambda(q) \rangle_{n\varepsilon'l'}. \quad (3)$$

λ is the transfer of angular momentum in the interaction, l the initial and l' the final angular momenta. $o_l = 2(2l+1)$ is the statistical occupation number of the initial state.

$\chi_{l'}^t(\varepsilon')$ is the partial DOS for angular momentum l' at atom t and for the energy ε' above Fermi level; $\langle j_\lambda(q) \rangle_{n\varepsilon'l'}$ is the matrix element of the spherical Bessel function of order λ between the radial parts of the initial and final states.

For anisotropic monocrystalline samples of low symmetry, formula (3) has to be extended as shown by Nelhiebel *et al.* [19].

Both expressions, for the case of a polycrystalline sample and for an anisotropic monocrystal can be calculated with the TELNES package which is an extension of the WIEN97 band structure code [20,21].

3 Structures

Lattice parameters, structure type and atom positions of the oxides V₂O₅, VO₂, V₂O₃ and VO studied are summarised in Table 1.

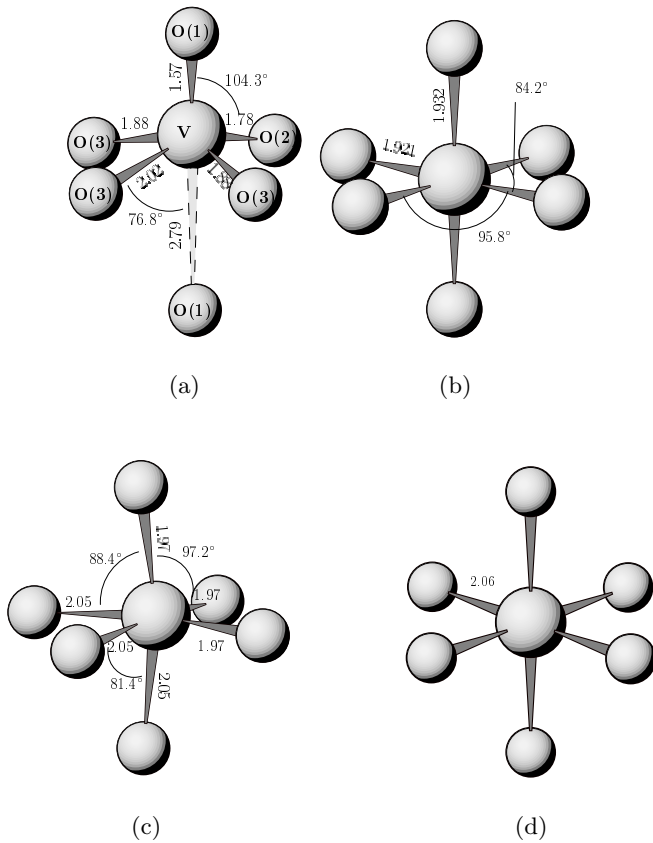


Fig. 1. Octahedron structures around V in V_2O_5 (a), VO_2 (b), V_2O_3 (c) and VO (d). The lengths are in Å.

A common structural feature of all the four compounds are the VO_6 octahedra consisting of six oxygen atoms at the corners and one vanadium atom in the centre. According to the structure types the form of the octahedron varies from a strongly distorted one (in V_2O_5) to a regular form with six equal V-O bonding lengths (in VO). The bonding V-O length increases with decreasing oxidation states of vanadium (Tab. 1 and Fig. 1).

In V_2O_5 the oxygen atoms are on three different sites. Each layer is composed of edge-sharing octahedra organised in zigzag lines; between two lines, octahedra are sharing corners and also two layers are connected by common corners [9, 22, 25].

VO_2 occurs in a monoclinic (distorted rutile) structure at low temperatures and a rutile structure at high temperature. Electron diffraction showed that the VO_2 we studied is in the metallic rutile modification. The VO_6 octahedron is less distorted than that in V_2O_5 (Fig. 1). The octahedra are arranged along edge-sharing lines parallel to the c -axis of the crystal, each turned to the other by 90 degrees with joined corners.

V_2O_3 has the rhombohedral corundum structure with less distorted VO_6 octahedron sharing corner and edges in a double chain structure.

VO has the rock-salt structure, consisting of perfect VO_6 octahedra with 6 equivalent V-O bonds.

4 Calculations and experiments

Calculations were performed using the full potential augmented planes waves package WIEN97 [21] and the TELNES program for simulations of ELNES spectra [20]. The core hole left by the excited electron was neglected and the magnetic properties of the compounds (spin-orbit coupling and spin-polarisation) were not taken into account in the present work. This simplification does not influence the calculation of the O- p density of unoccupied states, as will be discussed in the following. Relaxation of the structures was not performed since it does not really influence the DOS and thus the ELNES [13].

For the calculation, the number of k -points and the plane waves cutoff were increased until no changes were observable in the ELNES. VO was calculated with 35 k -points in the irreducible part of the Brillouin zone, a plane wave cutoff R_{kmax} of 8 (corresponding to an energy cutoff of 16.8 Ry) and the atomic spheres radius were 1.9 a.u. for both V and O. We took 60 k -points for V_2O_3 , an atomic sphere radius of 1.84 a.u. and R_{kmax} of 8 (energy cutoff of 17.9 Ry). 30 k -points were necessary for VO_2 , the atomic sphere radius was 1.8 a.u. for both V and O and the plane wave cutoff 8.5 (21 Ry). V_2O_5 was calculated with 84 k -points, a plane-wave cutoff of 8 (31 Ry) and atomic sphere radii of 1.5 a.u. for vanadium, 1.4 a.u. for O(1) and 1.8 a.u. for O(2) and O(3). The generalised gradient approximation (GGA) was used as exchange-correlation potential [26]. Test calculations on VO showed no noticeable differences when using the LDA approximation as was reported by Chakrabarati *et al.* for V_2O_5 [12]

For the EELS-measurements, vanadium oxides from Fluka Chemie GmbH are used. Samples were gently crushed with a mortar in carbon-tetrachloride. A drop of the solution with the crushed crystal powder was deposited on a holey carbon support film on a copper grid. All measurements were performed in a Philips CM 200 field emission transmission electron microscope equipped with a Gatan energy filter for EELS measurements. The microscope was operated at 200 kV. The energy resolution, estimated from the full-width at half maximum of the zero-loss peak, was 1 eV. All the EELS-measurements were recorded at the same experimental conditions (same convergence and collection angle, same beam energy, and the post-treatment of the spectra was performed the same way). The collection angle was 3 mrad and the illumination angle was 1.5 mrad. Under these experimental conditions, the effect of anisotropy in V_2O_5 is not significant [27].

5 Results

5.1 Density of states

The total DOS calculated for the four compounds are presented in Figure 2. The dotted line (at 0 eV) denotes the Fermi level. For V_2O_5 , the obtained band gap of 1.8 eV is smaller than the experimentally observed gap

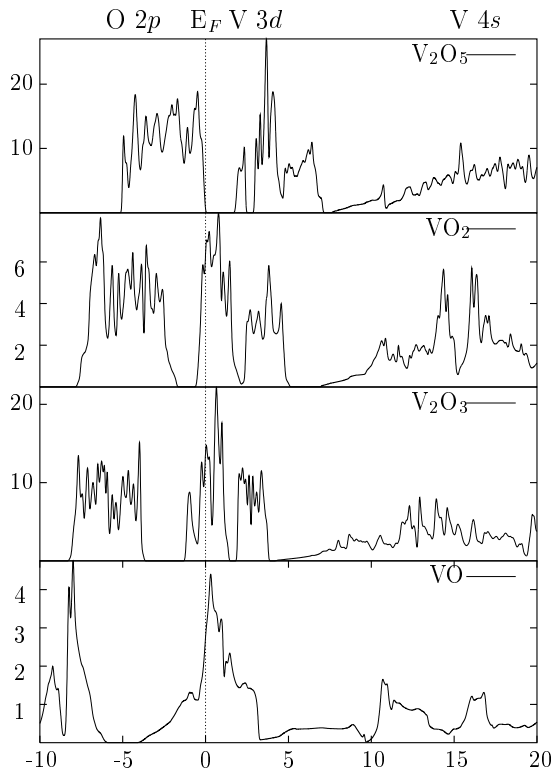


Fig. 2. Comparison of the total DOS of the 4 structures showing the changes in the DOS with increasing oxidation state. VO, V_2O_3 and VO_2 are metallic whereas V_2O_5 is an insulator. The DOS is plotted in states/eV versus energy in eV.

of 2.2 eV [11]. With increasing oxidation state, the valence band (VB) shifts towards the Fermi level. This is evident since the number of available electrons decreases as the oxidation state increases. According to the calculation, V_2O_5 is an insulator, VO_2 is a metal with a Fermi Level at the very bottom of the conduction band. In V_2O_3 and VO Fermi levels are in the conduction band, as is also found experimentally.

The compounds with good catalytic properties are all found to have V in an oxidation state between 5^+ and 4^+ . As a matter of comparison, there are 0.0396 occupied states in the conduction band per number of valence electrons for VO_2 , 0.0913 for V_2O_3 and 0.158 for VO. The total DOS compares well with previous results for V_2O_5 [12, 11], VO_2 [13, 5] and V_2O_3 [13, 7].

O $2p$ states are mainly situated below the Fermi level. However, because of hybridisation the symmetries are slightly mixed so that a small amount of O $2p$ is present above the Fermi level (otherwise no O K-edge would be visible in the spectra). For all compounds, the lower parts of the conduction band are dominated by V $3d$ states, while the higher parts contain V $4s$ states (Fig. 2).

Figures 3 to 6 show the partial d -DOS at the V site and the partial p -DOS at the O sites for the four compounds. As an example we additionally show in Figures 3 and 6 the V d -DOS splitted into its different components for V_2O_5 and VO respectively. Because of the octahedral en-

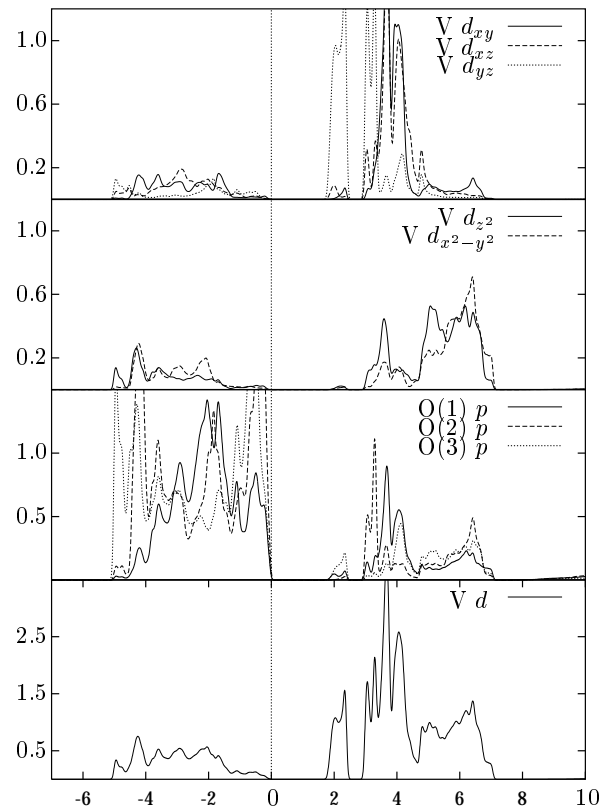


Fig. 3. d -projected DOS at the V site and p -projected DOS at the 3 O-sites in V_2O_5 in states/eV. Energy scale is in eV and the Fermi level E_F set to 0 eV. The local coordinate system corresponds to the one used by WIEN97 in which the x axis is in the direction of the V-O(1) ligand (parallel to the c axis of the crystal) and the y axis in the direction of the V-O(2) ligand.

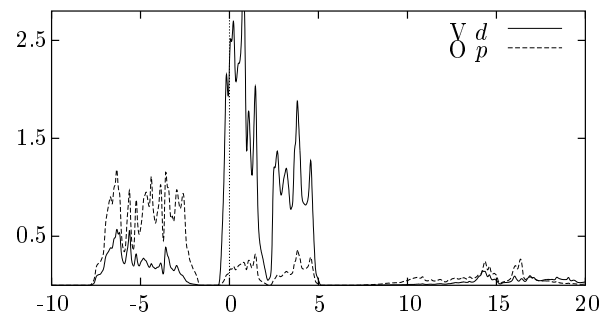


Fig. 4. d -projected DOS at the V site and p -projected DOS at the O site in VO_2 in states/eV. Energy is in eV and the Fermi level is set to 0 eV.

vironment of the vanadium and despite of the octahedron deformation, the crystal field splittings lead to separations of the lower part of the conduction bands into t_{2g} and e_g bands. e_g states are higher in energy and correspond to σ^* anti-bonds and t_{2g} are lower in energy correspond to π^* anti-bonding states.

For the 3 oxides with strong octahedral deformation, the splittings between e_g and t_{2g} are more important.

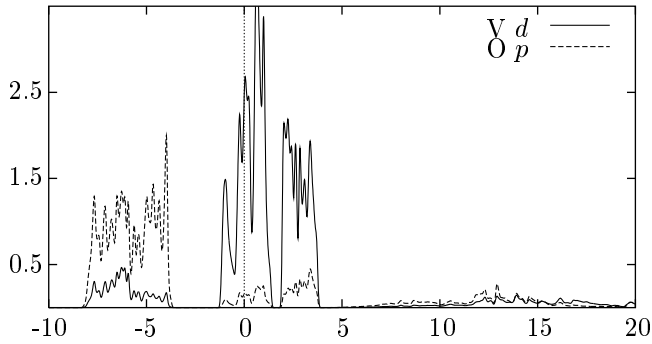


Fig. 5. d -projected DOS at the V site and p -projected DOS at the O site in V_2O_3 in states/eV. Energy is in eV and the Fermi level set to 0 eV.

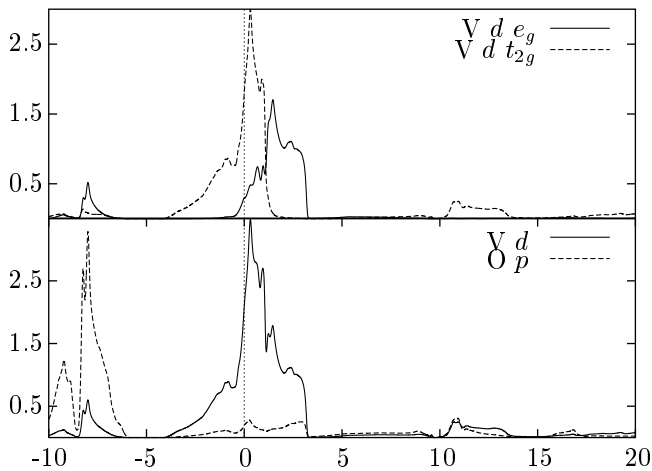


Fig. 6. d -projected DOS at the V site and p -projected DOS at the O-site in VO states/eV. Energy is in eV and the Fermi level set to 0 eV.

V_2O_5 exhibits an additional band splitting in the t_{2g} unoccupied states at about 2 eV above the Fermi level. As can be seen in Figure 3 this band mainly underlies an hybridisation between V d_{yz} and O(3) p states [28].

A detailed analysis of the hybridisations between the V d - and the O p -states was given by Eyert. The calculations of the site and angular momentum projected DOS of V_2O_5 are in good agreement with those done by Chakrabarati *et al.* [12] and Eyert *et al.* [11].

5.2 ELNES

The unoccupied O- p states are well suited for a comparison with experiment since they show up as a fine structure (ELNES) in the O-K ionisation edge. Figure 7 shows the O- p partial DOS for the four compounds broadened with a Gaussian of 1 eV FWHM. For comparison with ELNES experiments the DOS of V_2O_5 has been shifted to the left by 1.83 eV (the band gap). The DOS of the 3 inequivalent O atoms in V_2O_5 have been added and weighted by the number of atoms in the cell.

The changes in the DOS can be seen as a rigid shift of the valence band as the oxidation state changes from V^{5+}

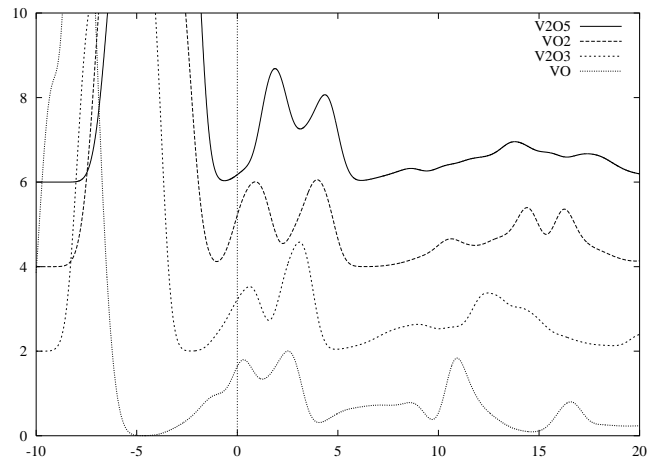


Fig. 7. p -projected DOS at the O site for the 4 compounds broadened with a Gaussian of 1.0 eV FWHM. The V_2O_5 DOS was shifted from 1.83 eV to the left in order to put the Fermi level at the bottom of the conduction band instead of the top of the valence band.

to V^{2+} and as a smaller shift of the structures in the conduction band. There is also an important modification in the relative weight of e_g and t_{2g} which can be attributed to differences in the local environment of the oxygen atoms: with decreasing oxidation state of vanadium the octahedral deformation is reduced and the O has more σ bonds with surrounding vanadium, thus increasing the σ (e_g) part and reducing the π (t_{2g}) part of the DOS.

All the four vanadium oxides were checked by electron diffraction in order to ensure that the EELS-spectra are taken from specimens with the structure type given in Table 1. The diffraction patterns of the four compounds are shown in Figure 8. The orientations have been determined using the "in" program of the EMS package by Stadelman [29]. They can be identified as patterns from V_2O_5 [001], VO_2 [110] V_2O_3 [211] and VO [100].

Additionally, diffraction patterns of each sample were recorded after each EELS measurement, in order to follow possible structural changes during the measurement since vanadium oxides tend to be reduced by electron beam [30] irradiation.

The experimental O-K ELNES, extracted from the EEL-spectra after background and multiple scattering correction [15], are shown in Figure 9 together with the simulated ELNES for comparison. The simulations take into account the matrix element as defined in formula 3. The instrumental broadening was modelled by a Gaussian of FWHM 1 eV, the core hole lifetime by a Lorentzian of 0.2 eV FWHM and the excited state life time by an energy-dependent Lorentzian of width $0.1E$ with E energy above the Fermi level. The tail of the vanadium L_{23} edge has not been removed from the experiment since the two edges are too close to each other to allow the conventional background fitting by a power-law. The background has therefore been removed in front of the V- L_{23} edge. For the simulation, the absolute energy position of the edge cannot be retrieved from the *ab initio* calculation because of

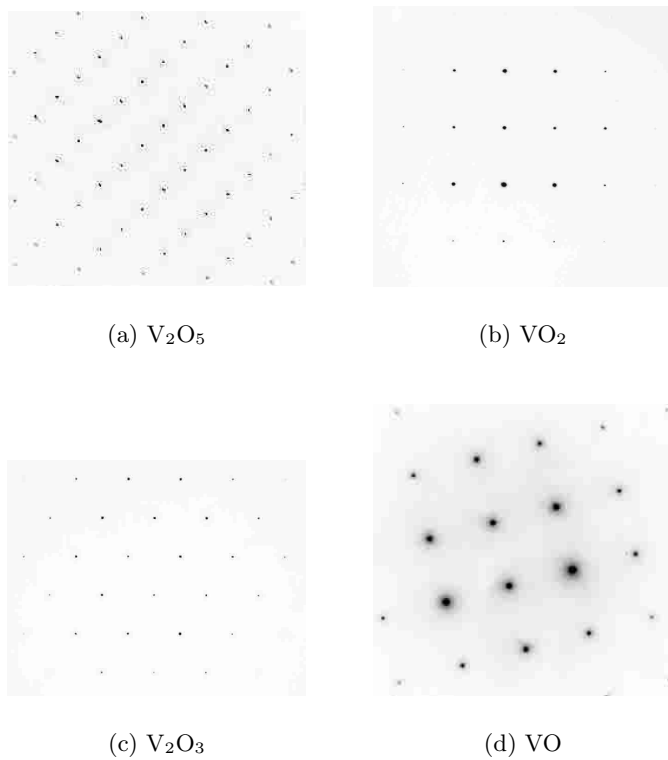


Fig. 8. Diffraction pattern of the four oxides, V_2O_5 in the [001] orientation, VO_2 in the [110] orientation, V_2O_3 in the [211] orientation and VO in the [100] orientation.

two reasons: the first is that the calculation is made in a ground state with occupied core level while a core hole will be created during the interaction process. A method for taking this into account would be the use of Slater's transition states where the core occupancy is set to 0.5 [31]. The second reason applies to V_2O_5 and is the well known fact that the DFT is not able to predict correct band gaps. Thus, for the comparison with experiments, the simulation has been aligned to the experiment at the first maximum of the O-K edge.

The agreement between theory and experiment is excellent. The apparent discrepancies in the relative heights of the e_g and t_{2g} peaks for V_2O_5 and VO_2 can be explained by the trailing edge of the V L_2 white line which superimposes the O-K ELNES and changes the relative heights of the e_g and t_{2g} structures. For VO and V_2O_3 , the part of the V L_{23} edge situated below the O K-edge comes from the $2p$ to $4s$ transition. Since the $4s$ DOS has only little structure, the V L edge will not influence the positions and intensities of the structures. The t_{2g} and e_g contributions in the O-K edge are only well separated in VO_2 (Fig. 9). In V_2O_5 and V_2O_3 , the two peaks overlap but can still be recognised. From the unbroadened O- p DOS (Figs. 3 to 6) it is clear that the apparent overlapping of the e_g and t_{2g} contributions to the ELNES of V_2O_5 , VO_2 and V_2O_3 is due to the broadening of the spectral features. Due to the overlapping of the t_{2g} and e_g bands in VO , a unique

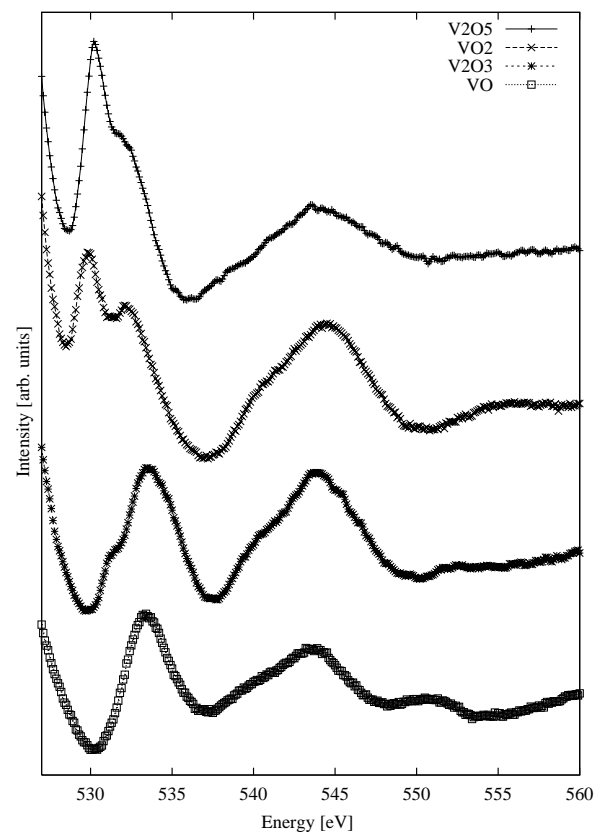
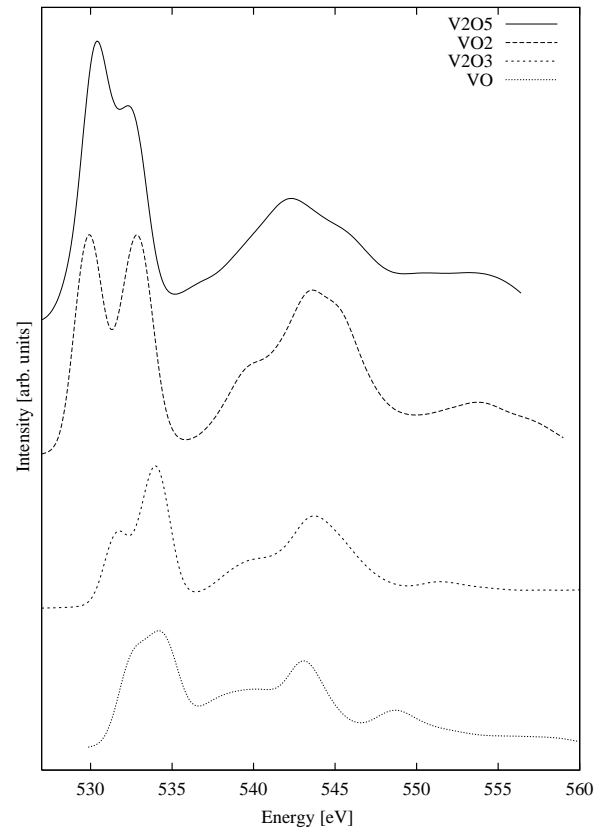


Fig. 9. Simulated (above) and experimental (below) O-K edges. The experimental spectra are calibrated in energy and the calculated spectra were aligned to the experiment at the first maximum.

assignment of transitions to these bands in the oxygen K edge is difficult.

The differences between the broadened O-*p* DOS (Fig. 7) and the O-K ELNES (Fig. 9) can be attributed to 3 phenomena: first of all the part of the DOS situated below the Fermi level is not visible in the ELNES; this will cut a small part of the t_{2g} peak in the metals and therefore reduce the t_{2g} contribution to the spectra. A second effect is based on the matrix element (Eq. 3) between the radial parts of the initial and final states which slightly changes the peak heights. Also the additional core-hole and excited lifetime Lorentzian broadening are not negligible.

Nevertheless, from a comparison between the occupied and unoccupied O-*p* DOS (Fig. 7) and the O-K ELNES (Fig. 9) it is clear that the important changes in the weighting of the e_g and t_{2g} peaks in the ELNES reflects changes in the O-*p* DOS and not the shift of the Fermi level. The decreasing e_g/t_{2g} ratio is well visible in the *p* projected DOS at the O site and plays a much more important role in the changes of the ELNES than the shift of t_{2g} states below Fermi level.

Good agreement between simulation and experiment is also achieved in the energy regions of transitions to O 2*p* and V 4*s* mixed states (538–555 eV).

The very narrow band in V₂O₅ lying at 2 eV can hardly be seen as a shoulder on the left of the t_{2g} states in the broadened O-*p* DOS (Fig. 7) due to the energy broadening. This shoulder is no more visible in the ELNES (Fig. 9) where additional broadening was applied. However the continuous improvement of electron microscopes and spectrometers and the promising development of monochromators on field emission guns which should allow a resolution of about 0.1 to 0.2 eV can let us hope that this effect could be detectable in the near future [32]. Since the materials interesting for catalysis are situated between V₂O₅ and VO₂, and since this additional splitting of the DOS is the main difference between the two materials associated with octahedral deformation, such investigations would be of great interest. This narrow band is well visible in the O-K edge of V₂O₅ recorded by NEXAFS spectroscopy [33].

6 Conclusion

We have shown that the ELNES of the O-K edge in vanadium oxides can be well reproduced with band structure calculations based on the GGA approximation, even without taking the spin-orbit coupling into account.

Independent of the distortion of the octahedra, both contributions e_g and t_{2g} are visible in the density of states of all oxides. The Fermi level shifts only slightly with decreasing oxidation state while the fine structures within the O-*p* band change strongly from V₂O₅ to VO. The differences in ELNES can be traced back to the different weighting factors of the two main contributions e_g and t_{2g} . Changes in the weighting between e_g and t_{2g} transitions could be attributed to changes in the local octahedral environment of the vanadium and not to shifts of the Fermi level.

Our study shows that the simple view of an ionic crystal with vanadium having exactly single valence state is not strictly true since the hybridisation between O 2*p* and V 3*d* states is very significant.

The demonstrated sensitivity of ELNES makes it a promising method for the detection of intermediate phases even in microscopic specimens thanks to the excellent spatial resolution of the TEM.

This work was supported by SFB 546 of the Deutsche Forschungsgemeinschaft and by the Austrian Science Fund (project PHY14038). We would like to thank K. Hermann (FHI-Berlin) and J. Luitz (Vienna University of Technology) for instructive discussions.

References

1. M. Abbate, *Brazilian J. Phys.* **24**, 785 (1994)
2. H. Abe, M. Terauchi, M. Tanaka, S. Shin, *Jpn J. Appl. Phys.* **37**, 584 (1998)
3. H. Abe, M. Terauchi, M. Tanaka, S. Shin, Y. Ueda, *Jpn J. Appl. Phys.* **36**, 165 (1997)
4. E. Caruthers, L. Kleinmann, H.I. Zhang, *Phys. Rev. B* **7**, 3753 (1973)
5. E.Z. Kurmaev, V.M. Cherkashenko, Y.M. Yarmoshenko, S. Bartkowskis, A.V. Postnikov, M. Neumann, L.C. Duda, J.H. Guo, J. Nordgren, V.A. Perelyaev, W. Riechelt, *J. Phys. Cond. Matt.* **10**, 4081 (1998)
6. K. Hermann, A. Chakrabarati, A. Haras, M. Witko, B. Tepper, *Phys. Status Solidi (a)* **187**, 137 (2001)
7. L.F. Mattheiss, *J. Phys. Cond. Matt.* **6**, 6477 (1994)
8. D.W. Bullett, *J. Phys. C* **13**, L595 (1980)
9. L. Fiermans, P.C.W. Lambrecht, L. Vandenbroucke, J. Vennik, *Phys. Status Solidi (a)* **59**, 485 (1980)
10. J.C. Parker, D.J. Lam, Y.N. Xu, W.Y. Ching, *Phys. Rev. B* **42**, 5289 (1990)
11. V. Eyert, K.-H. Höck, *Phys. Rev. B* **57**, 12727 (1998)
12. A. Chakrabarati, K. Hermann, R. Druzinic, M. Witko, F. Wagner, M. Petersen, *Phys. Rev. B* **83**, 10583 (1999)
13. K. Hermann, M. Witko, in *The Chemical Physics of Surfaces*, Vol. 9, *Oxide Surfaces*, edited by D.P. Woodruff (Elsevier, New-York, 2001), pp. 136–198
14. X.W. Lin, Y.Y. Wang, V.P. Dravid, P.M. Michalakos, M.C. Kung, *Phys. Rev. B* **47**, 3477 (1993)
15. R.F. Egerton, *Electron Energy Loss Spectroscopy in the electron microscope* (Plenum Press, 1986)
16. P. Rez, J. Bruley, P. Brohan, M. Payne, L.A.J. Garvie, *Ultramicroscopy* **59**, 159 (1995)
17. P. Rez, J.R. Alvarez, C. Pickard, *Ultramicroscopy* **78**, 175 (1999)
18. H.A. Bethe, *Ann. Phys.* **5**, 325 (1930)
19. M. Nelhiebel, P.-H. Louf, P. Schattschneider, P. Blaha, K. Schwarz, B. Jouffrey, *Phys. Rev. B* **59**, 12807 (1999)
20. C. Hébert-Souche, P.-H. Louf, P. Blaha, M. Nelhiebel, J. Luitz, P. Schattschneider, K. Schwarz, B. Jouffrey, *Ultramicroscopy* **83**, 9 (2000)

21. P. Blaha, K. Schwarz, J. Luitz, *WIEN97, A Full Potential Linearized Augmented Plane Wave Package for Calculating Crystal Properties* (Karlheinz Schwarz, Techn. Universität Wien, Austria, 1999)
22. R. Enjalbert, J. Galy, *Acta Cryst. C* **42**, 1467 (1986)
23. M.G. Vincent, K. Yvon, J. Ashkenazi, *Acta Cryst. A* **36**, 808 (1980)
24. R.E. Loehman, C.N.R. Rao, J.M. Honig, *J. Phys. Chem.* **73**, 1781 (1969)
25. J. Haber, M. Witko, R. Tokarz, *Appl. Catalysis A: General* **157**, 3 (1997)
26. J.P. Perdew, K. Burke, M. Ernzerhof, *Phys. Rev. Lett.* **77**, 3865 (1996)
27. D.S. Su, C. Hébert, M. Willinger, R. Schlögl, *Ultramicroscopy* (submitted)
28. M. Willinger, *Investigation of the oxygen K-edge fine structure in vanadium oxides*, Diploma thesis, Vienna University of Technology, May 2001
29. P. Stadelmann, *Ultramicroscopy* **21**, 131 (1987)
30. D. Su, M. Wieske, E. Beckmann, A. Blume, G. Mestl, R. Schlögl, *Catalysis Lett.* **75**, 81 (2001)
31. J.C. Slater, *The self-consistent Field for Molecules and Solids, Quantum theory of Molecules and Solids*, Vol. 4 (McGraw Hill, 1974)
32. D.S. Su, H.W. Zandbergen, G. Kothleitner, P.C. Tiemeijer, M.H. Hävecker, C. Hébert, A. Knop-Gericke, B.H. Freitag, F. Hofer, R. Schlögl, *Ultramicroscopy* (submitted)
33. E. Goering, O. Müller, M. Klemm, M.L. denBoer, S. Horn, *Phil. Magazine B* **75**, 229 (1997)